LIP-STUDENTS-23-30

Muon Neutrino Energy Reconstruction in SND@LHC

Pedro Teigão[1,a]

[1] *Instituto Superior Técnico, Lisboa, Portugal*

Project supervisors: Nuno Leonardo, Guilherme Soares and Cristóvão Vilela

July 2023

Abstract. A method was studied that aims at determining the energy of muon neutrinos undergoing charged-current interactions in the SND@LHC experiment. The paper discusses various fundamental properties of the decay process, such as the conservation of energy and momentum. By estimating the muon energy, the neutrino energy can be inferred. A practical method is thus proposed and implemented to determine the energy of muon neutrinos in charged-current interactions, and the associated uncertainties are estimated for different scenarios.

KEYWORDS: Neutrinos, LHC, Detector

1 Introduction

The Large Hadron Collider (LHC) is a world-renowned particle accelerator located near Geneva, Switzerland, where protons collide at high energies with each other, in order to investigate the characteristics of fundamental interactions. Recently, there has been interest in studying neutrinos produced in the LHC collisions.

With no electric charge and extremely small mass, neutrinos are subatomic particles that interact very feebly. They are created in particle accelerators like the LHC, in nuclear processes that take place in the Sun and other astronomical sources, nuclear reactors and cosmic rays interactions with the atmosphere. As a result of their weak interactions with matter, neutrinos are incredibly elusive and challenging to find. Therefore, in order to study these particles, the SND@LHC experiment was proposed to detect for the first time neutrinos produced in proton-proton collisions at the LHC.

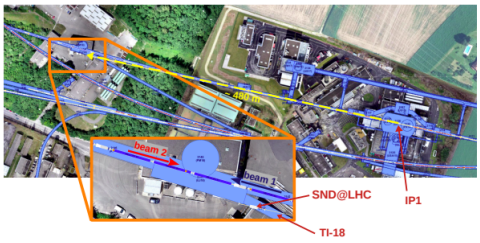

(a) Location of the Detector

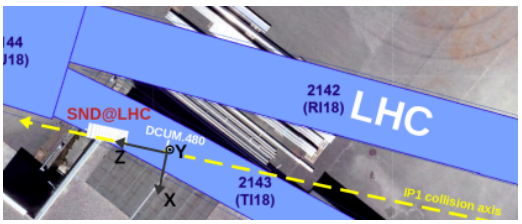

(b) Coordinate System Visualisation

Figure 1: Location and Coordinates

2 The SND@LHC Experiment

2.1 Location and Coordinate System

The SND@LHC detector is placed in the TI-18 service tunnel located 480 m away from the ATLAS interaction point (IP1). The majority of particles interacting with the detector come from beam crossings at IP1.

The coordinate system has its origin located at 480 meters away from the IP1 beam collision axis. The Z axis is aligned with the beam collision axis, this axis extends from IP1 towards the TI-18 tunnel.The y axis is perpendicular to the LHC machine plane and points upwards. Meanwhile the x axis is perpendicular to both the Y and Z axes. The detector is strategically positioned slightly off-axis from the collision axis to capture neutrinos resulting from the decay of charm quarks. Figure 1 better illustrates the detector location and coordinate system.

2.2 Components of the detector

The SND@LHC detector, shown in fig.2 is specifically designed to carry out precise measurements using high-energy neutrinos ranging from 100 GeV to a few TeV. These neutrinos are generated at the LHC and are detected in the forward pseudo-rapidity[1] region, which lies between $7.2 < \eta < 8.4$. The detector is capable of accurately identifying neutrino interactions of all three flavors with a high level of efficiency.

The detector is composed of three main systems: the veto, emulsion target, and muon systems.

Positioned in front of the target region, the veto detector (Veto) is comprised of two vertically shifted planes consisting of seven scintillating bars measuring $42 \times 6 \times 1$ cm³. the Veto is used to determine whether these interactions came from charged or neutral particles.

[a] e-mail: pedro.teigao@tecnico.ulisboa.pt

[1] Pseudorapidity is a quantity commonly used in high-energy physics to describe the angle of a particle's trajectory with respect to the beam axis.

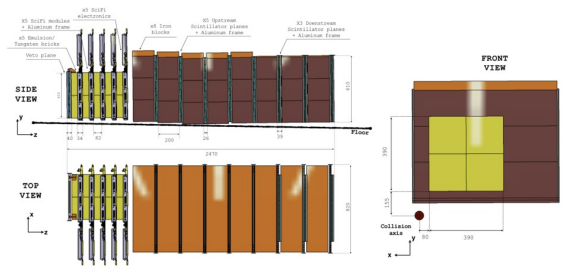

Figure 2: Schematic of Detector and Coordinate System

The Emulsion Target (ECC) is located downstream of the Veto and is composed of 5 walls. Each wall is made of 4 emulsion bricks, consisting of 60 emulsions films interleaved with 59 layers of 1 mm tungsten plates. When charged particles pass through the emulsion films, they create a track that captures their position. These films can be developed later, providing precise information on the trajectory and characteristics of the occuring interaction.

The Muon System is positioned after the Emulsion Target in the detector setup. It serves two primary functions: the identification of muons, which is crucial for detecting muon neutrino, and it operates as a Hadronic Calorimeter, capable of measuring the energy of hadronic showers. The Muon System comprises a total of nine planes, with the first five planes referred to as Upstream (US) planes and the remaining three planes as Downstream (DS) planes, and a last simpler 9^{th}. The system is constructed by interleaving eight scintillating planes with 20 cm thick iron slabs. The Upstream planes consist of ten horizontal bars that aid in vertically locating particles by identifying which bar and at what height it was triggered. On the other hand, the Downstream planes offer higher spatial resolution through two layers of thinner bars: one arranged horizontally and the other arranged vertically. This arrangement allows for more precise particle localization, like the muon, in a two-dimensional plane. Additionally, there is an extra downstream plane, which consists of a single vertical layer without an iron slab preceding it.

3 Motivation

Plans are underway to install a magnet spectrometer that when a muon passes through it we can determine is momentum using its curvature. Until then, the energy of muon neutrinos must be inferred using only information related to the hadronic system and the scattering angle of the muons. There is a particular interest in muon neutrinos since they provide the biggest amount of expected interactions, and although the muon is easily identifiable due to its penetrating trait this also makes it so that a calorimeter cannot measure its energy. In this project, a method for inferring the neutrino energy by balancing the hadronic and muon momenta on a plane transverse to the neutrino direction is explored.

4 Neutrino Interactions

The scattering of neutrinos occurs through the exchange of a W or Z boson (fig.3). This scattering process provides valuable insights into the properties of the neutrino. By examining the products of the neutrino interaction we can determine its momentum and energy through the principles of energy and momentum conservation. Additionally, the flavor of the neutrino can be identified by detecting the charged lepton produced during the interaction.

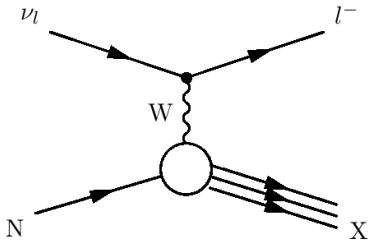

Figure 3: Charged Current Neutrino Scattering

5 Neutrino Interaction Simulation

Using Genie [1], a software framework for experimental neutrino physics, it is possible to simulate neutrino interaction events. The detailed description of each event is saved to a ROOT TTree [2] in the Genie Summary Tree (gst) format.

5.1 Event Distribution Simulation

Based on the current conditions of the experiment, simulations of events were conducted using the expected energy spectrum. Figure 4 illustrates the total number of simulated events, broken down by neutrino flavours.

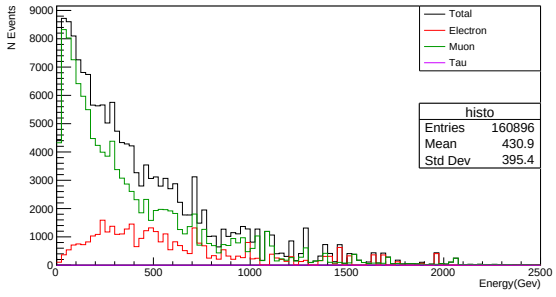

Figure 4: Simulated Neutrino Energy Spectra

From this simulation, it can be concluded that the main number of events expected to be obtained in the range of

operation of the detector are muon neutrino and electron neutrino interactions. It is also possible to conclude that the lower the energies in that interval, the more likely the event is muon-neutrino related.

In reality, the number of simulated events is much higher than the number of expected events, so a proportionality scale correction has to be applied in order to have a real perspective of the magnitude of the different effects studied. The simulated data set analysed in this project corresponds to $2 \cdot 10^4\ fb^{-1}$, therefore a scale factor of 0.0125 needs to be applied to the histogram (fig.5). With this new scale we are expected to encounter around 2007 events where 459 are electron-neutrino related and 1493 are muon-neutrino related.

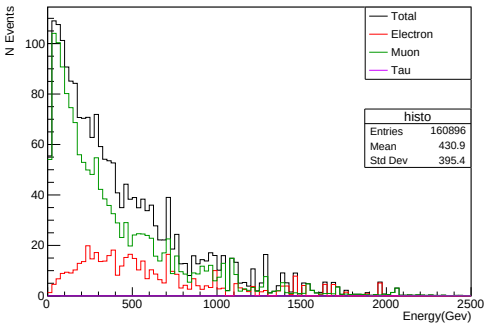

Figure 5: Scaled Simulated Neutrino Energy Spectra

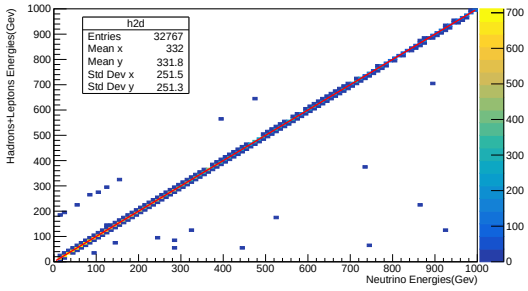

Figure 6: Energy of the Incoming Neutrino vs Products

5.2 Energy and Momentum Conservation

5.2.1 *Conservation of Momentum and Energy in the Decay*

In order to validate the simulated data, we analysed if the simulated data obeys the expected conservation laws. Starting with the energy, the total energy of the resulting products (lepton and hadrons) was plotted in fig. 6 as a function of the incoming neutrino energy in a 2D histogram with a function y=x in red.

From fig. 6, it is evident that the conservation of energy is upheld since the majority of events closely align with the red line. Additionally, the presence of only a few outliers indicates a minimal deviation from the expected energy conservation. These outliers can be attributed to the energy correction applied, as we ignored the presence of protons and neutrons in the final state and impose that they had no momenta. Additionally, we disregarded the rare appearance of "nuclear fragments" in the final state of events

Applying the same analysis method to the three different momentum coordinates (P_x, P_y, P_z), the conclusions are similar to what was previously stated, as shown in figs. 7 to 9.

There is conservation of momentum along all three axes, but the variation in the graphs can be attributed to the environmental conditions surrounding the detector. Considering that the particle flux and the detector are slightly aligned with the z-axis, it is expected that the momentum values along this axis would be higher. On the other hand, the x and y axes exhibit lower values due to the placement of the detector in the reference frame, even thought the majority of events have near null x and y momenta this placement of the detector makes it so that the incoming neutrinos and decay products present a tendentiously positive momenta in y and tendentiously negative momenta in x. Also it is worth noting that the difference in results by a factor of 2 stems from the detector's position, which is located 15 cm above the origin along the y-axis and 8 cm away from the origin in the negative direction of the x-axis.

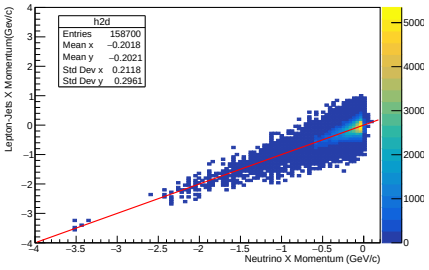

Figure 7: Momentum of the Incoming neutrino vs Products in x

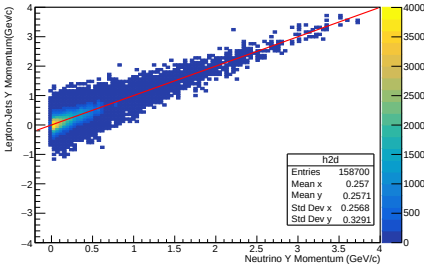

Figure 8: Momentum of the Incoming neutrino vs Products in y

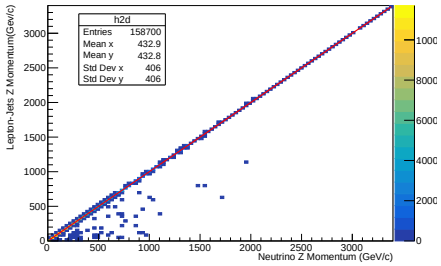

Figure 9: Momentum of the Incoming neutrino vs Products in z

5.2.2 *Transverse Plane Momentum Relation*

To reconstruct the energy of the incoming neutrino, it is crucial to determine the energies and momenta of the decay products.

As it was previously seen, the total momentum is conserved and the neutrino has non zero momentum in the x and y direction. For this analysis we consider the transverse momentum as the momentum in the perpendicular plane to the neutrino momentum direction, then we can represent a neutrino interaction with the schematics shown in fig. 10

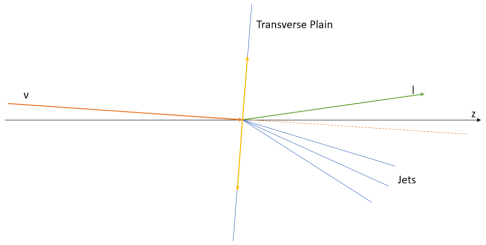

Figure 10: Interaction topology and transverse plane

Calculating and plotting the transverse momentum for the charged lepton and total transverse momentum for jets, the result is the histogram in fig. 11

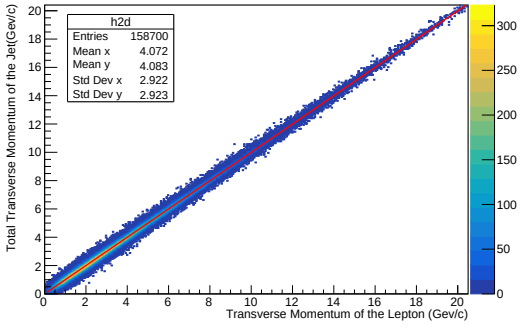

Figure 11: Conservation of the Transverse Momentum

It can be seen that the total transverse momentum is conserved. However, if we can determine the momentum and energy of the jet, along with the directions of both the products and the neutrino, it becomes possible to ascertain the lepton's energy and momentum using the proprieties previously discussed.

6 Reconstruction of the Neutrino Energy

In order to determine the muon momentum and energy, it is necessary to take into account that the total transverse momentum by default is zero. Hence, if we know the direction of the lepton, the direction of the neutrino and jet momentum it is possible to determine the muon momentum and energy, and consequently, the neutrino energy.

6.1 Momentum

The direction of the neutrino can be inferred by utilizing information about its interaction point within the detector and its average production point at IP1. Additionally, assuming that all information about the jet momentum is known and using the condition of zero total transverse momentum, we can determine the momentum of the associated lepton. The plot shown in fig. 12 displays the magnitude of the reconstructed momentum for the muon as a function of the expected value. Based on the observations from our plot, it can be concluded that the lepton momentum can be determined using this method.

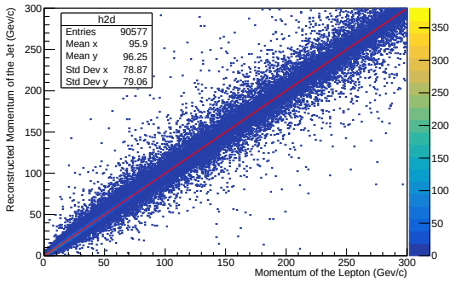

Figure 12: Momentum of the Lepton vs Reconstructed Momentum of the Lepton

With the reconstructed lepton momentum we can determine the total product momentum in the neutrino direction and by applying the principles of momentum conservation we can calculate the neutrino momentum. The resulting was plotted in fig. 13, where the calculated momentum was represented as a function of the expected value:

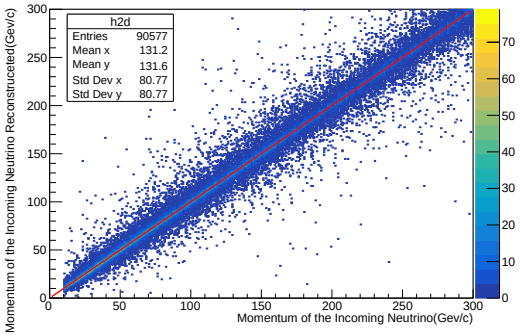

Figure 13: Momentum of the Incoming Neutrino vs Reconstructed Momentum of the Neutrino in the Neutrino Direction

6.2 Energy

Finally, the energy of the muon can be determined using the relativistic expression for energy. The simulated value was plotted as a function of the expected one, as show in fig. 14.

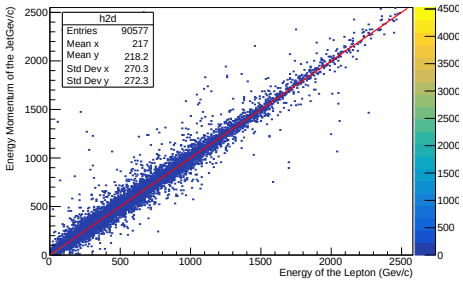

Figure 14: Energy of the Muon vs Reconstructed Energy of the Muon

With the energy of the muon, we can plot the resulting total energy of the products as a function of the incoming neutrino energy (fig. 15). Once again, conservation of energy is observed.

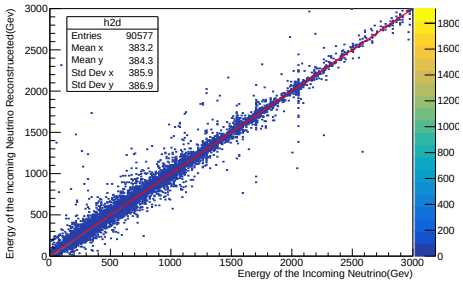

Figure 15: Energy of the Incoming Neutrino vs Reconstructed Energy of the Incoming Neutrino

6.3 Intrinsic Uncertainty

Having determined that the conservation of transverse momentum method can be used to determine the energy and momentum of the muon and muon neutrino, we can determine the intrinsic uncertainty of the method. This is evaluated as the relative difference between generated and estimated neutrino energy, and is shown in fig. 16.

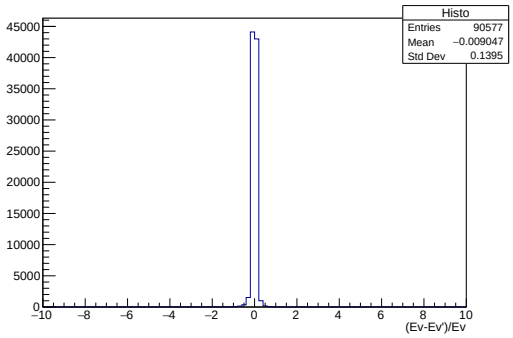

Figure 16: Standard Deviation for the Energy

From the plot we obtain that the reconstruction has an intrinsic uncertainty 14%. This deviation stands from the fact that the interaction occurs in the tungsten core, a heavy nucleus, and this can lead to loss of energy and momentum that our method does not have in consideration. Despite that, our method should be viable to calculate energies and momenta in these interactions.

7 Uncertainty in the Measurement

Until now, we have assumed that the total jet momentum and angles are precisely known. However, in reality, this assumption is far from accurate. Jets are comprised of numerous hadrons, making it challenging to accurately determine their momentum and energy. Furthermore, these hadrons can interact with the particles comprising the detector, further complicating their reconstruction. Consequently, the precise measurement of the total jet momentum and direction, as previously assumed, is unattainable. The same can not be said about the angles between the neutrino and the lepton, where it is possible to discover the angles more accurately, although it always has an uncertainty associated to it.

To understand the impact of this uncertainties on the reconstruction process, we introduced an uncertainty factor for the total jet momentum and angles. Using a Gaussian distribution we introduced an uncertainty of 0%, 10%, 20% and 30% of the expected value to the jet momentum. For the angle between the neutrino and the total jet direction (ϕ) we will assume a standard deviation of 0º, 0.05º, 0.125º, 0.25º,0.5º and 1º following the same distribution. If we apply the same method as in section 6 and examine

combinations of these scenarios (fig.17), we can assess how the intrinsic uncertainty of the neutrino energy reconstruction is influenced.

Table 1 shows the combination of the uncertainties previously mentioned and the associated standard deviation for the energy of the neutrino.

ϕ/Jets	0%	10%	20%	30%
0º	0.14	0.17	0.27	0.38
0.05º	0.14	0.18	0.28	0.39
0.125º	0.15	0.20	0.30	0.41
0.25º	0.17	0.23	0.34	0.44
0.5º	0.23	0.30	0.40	0.51
1º	0.38	0.46	0.56	0.68

Table 1: Estimated neutrino energy uncertainty for different ϕ and jet energy uncertainty values

From table 1 it is evident that as the uncertainty increases the deviation also increases. Based on these findings, we can conclude that the angle has a great influence over the uncertainty, therefore it is crucial that the accuracy of the jet direction is as precise as possible.

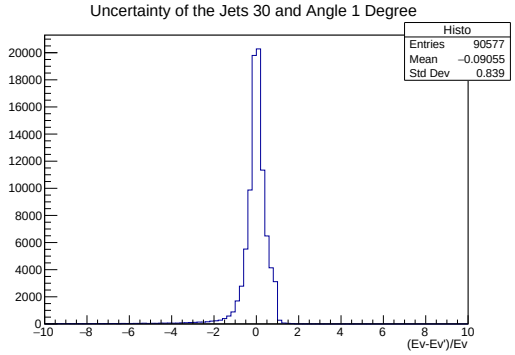

Figure 17: Example neutrino energy resolution distribution obtained with the method

8 Conclusions

Measuring the neutrino energy is a crucial point in the SND@LHC program. During Run 3 of the LHC the experiment will not have the capability to directly measure the momentum of the muon produced in the ν_μ interactions. We have shown that reconstructing it through the hadronic jet properties is feasible, and if we use the current capabilities of the detector, accurately determining the momentum and energy of muon neutrinos based on jets is challenging. The expected uncertainty associated with the jets is relatively high, at around 20% [3]. Our study suggests that for this baseline, the minimum uncertainty associate with the neutrino energy measurement would be of 27%, assuming perfect reconstruction of the jet angle. Also the uncertainty in the reconstruction of the jet angle must be lower than 0.25º for this method to be feasible. Further studies will be developed in methods to determine the jet angle .

On a last note, once the magnet system is installed and we are able to directly measure the muon momentum, we can invert the transverse plane method and use the muon to facilitate the reconstruction and energy calibration of the jets.

References

[1] C. Andreopoulos, C. Barry, S. Dytman, H. Gallagher, T. Golan, R. Hatcher, G. Perdue, J. Yarba, arXiv preprint arXiv:1510.05494 (2015)

[2] F. Rademakers, R. Brun, Linux Journal **51**, 27 (1998)

[3] G. Acampora, C. Ahdida, R. Albanese, C. Albrecht, A. Alexandrov, M. Andreini, N. Auberson, C. Baldanza, C. Battilana, A. Bay et al., "Journal of Instrumentation" (2022)

[4] L. Garren, I. Knowles, T. Sjöstrand, T. Trippe, The European Physical Journal C, Particles and Fields. **15**, 205 (2000)